

Stabilization by Urea during Thermal Unfolding-Mediated Aggregation of Recombinant Human Interleukin-1 Receptor (Type II): Does Solvation Entropy Play a Role?

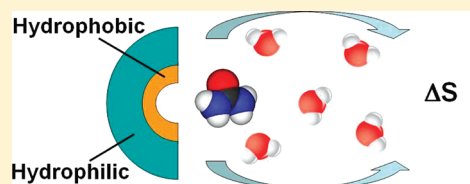
Richard L. Remmele, Jr.,[†] Jian Zhang-van Enk,^{*,‡} Duke Phan,[§] and Lei Yu[‡]

[†]MedImmune, 319 North Bernardo Avenue, Mountain View, California 94043, United States

[‡]Amgen Inc., One Amgen Center Drive, Thousand Oaks, California 91320-1799, United States

[§]Amgen Inc., 1201 Amgen Court West, Seattle, Washington 98119-3105, United States

ABSTRACT: The protein denaturing properties of urea are well-known and still the subject of debate. It has been noted that in some cases where urea concentrations are relatively low stabilization is afforded against aggregation. An explanation for this unusual effect has seemingly remained elusive. Evidence is offered to propose urea stabilization is related to its influence on the solvation property of the protein molecules when in contact with an unfolded hydrophobic surface that tends to increase the entropy of the local aqueous solvent. This property of urea is expected to lower the entropic driving force of unfolded-mediated aggregation despite the increase in enthalpy. The data presented from toluene transfer experiments into 2 M urea + 0.1 M sodium phosphate solutions showed that the solvation free energy change was negative up to ~ 75 °C. The associated $\Delta\Delta H$ was positive, leading to the conclusion that entropy drives the solvation process within the temperature domain from $\sim 20^\circ$ to 75 °C. Using thermodynamic parameters from the toluene solvation experiments, it was possible to accurately determine the T_m shift of recombinant human interleukin-1 receptor type II (rhIL-1R(II)). Heating experiments above the apparent T_m in the same urea/phosphate solution support the thesis that urea inhibits the entropy-driven aggregation process of rhIL-1R(II), adding yet another molecule to the list of low urea concentration stabilized molecules.



INTRODUCTION

Understanding how different chemical agents can affect solvent and protein properties is important for defining a rationale of protein stabilization.¹ Some agents can stabilize proteins by being excluded from the protein–solvent interface,^{2,3} while others can stabilize by nonspecific binding.⁴ Yet, a contradictory effect concerns how a protein denaturant can seemingly stabilize some protein systems against aggregation at relatively low concentrations (considered to be subdenaturing). For example, there have been several instances reported in the literature where urea exhibited a protein-stabilizing influence at low concentrations.^{5–8} Debates over urea's ability to stabilize proteins at relatively low concentrations have focused on its interactions with the solvent and with nonpolar protein side chains.^{7,9} It is well-known that most nonpolar solutes (with the exception of methane and ethane) have greater solubilities in urea aqueous solutions than in water alone.^{10,11} It has been suggested that the presence of urea decreases the hydrophobic effect by favorable hydrophobic solute–urea interactions as opposed to more unfavorable hydrophobic solute–water interactions.¹² Thus, a decrease of the hydrophobic effect by direct interaction of urea with hydrophobic side chains of a protein is one possible mechanism of protein stabilization. Another proposed possibility is that urea may impart a stabilization influence by how it affects the solvent structure and/or solvation entropy.^{13–16} Urea has been reported to

possess properties that favorably increase the entropy of water.^{17,18}

There has been evidence provided at concentrations of urea ≤ 2 M that urea interactions with proteins are generally weak.¹⁹ It has been suggested that at low urea concentrations the primary influence appears to impact solvent structure rather than protein unfolding.²⁰

When a protein unfolds, the exposure of a hydrophobic surface to the solvent can result in hydrophobically associated aggregates.^{21–24} The free energy threshold between the native and unfolded states is within 0.3–25 kcal/mol for most protein systems.^{25–28} Because this is a relatively small energy barrier to overcome, small populations of proteins (or ensembles) can occupy an unfolded state as governed by the thermodynamics of the solution at temperatures well below the unfolding transition. It is not unreasonable to assume that when the hydrophobic surface of a protein becomes exposed by unfolding (to whatever extent) that there will be a thermodynamic tendency to remove it from the solvent either by refolding (hydrophobic collapse) or by unfolded protein-mediated associations that displace solvent molecules from the hydrophobic surface. In the latter case, protein aggregates can result.

Received: January 12, 2012

Revised: April 10, 2012

Published: May 9, 2012



Here we consider the influence of urea at relatively low concentrations (~ 2 M) to inhibit unfolded-mediated aggregation for recombinant human interleukin-1 receptor type II (rhIL-1R(II)) at conditions above the T_m . Additionally, this study will examine the role of solvation entropy in solutions with and without urea using toluene as a hydrophobic probe to gain some perspective of the relative solvent entropic force that drives unfolded proteins together. Finally, a mechanism will be proposed based upon the findings of the experimental results.

MATERIALS AND METHODS

Purified rhIL-1R(II) was obtained as a bulk drug concentrate (~ 10 mg/mL) in a phosphate-buffered saline (PBS) solution (20 mM sodium phosphate (pH 7.4), 150 mM NaCl) obtained from Immunex Corporation (now Amgen, Inc.). The protein, expressed in Chinese hamster ovary (CHO) cells, was approximately 20% glycosylated with a molecular weight of ~ 38 kDa. Protein concentrations for case studies were determined spectrophotometrically at 280 nm using an experimentally determined molar extinction coefficient of 1.61 mL/mg cm.

All chemicals used in the experiments were of reagent grade quality or better. Ultra pure urea (99.9%) was purchased from J.T. Baker (Phillipberg, NJ). Anhydrous toluene (99.8%) and sodium phosphate (99.0%) were obtained from Alfa Aesar (Ward Hill, MA) and EMD chemicals (Gibbstown, NJ), respectively. The *n*-butanol (99.9%) was obtained from Sigma-Aldrich (St. Louis, MO).

The toluene stock solution for absorbance calibration was prepared by weighing 0.5029 g of toluene and dissolving it in 50 mL of *n*-butanol (in a 50 mL volumetric flask). Corresponding toluene standard solutions were prepared as a series of dilutions of the stock solution, and a linear calibration of the concentration as a function of absorbance at 260 nm (λ_{\max} for toluene absorbance) was determined and used to measure aqueous concentrations of urea for the equilibrium solubility and DSC measurements (further described below). Water and *n*-butanol blanks were subtracted from aqueous samples and calibration standard measurements, respectively.

PROTEIN THERMOSTABILITY STUDY

Near-UV Circular Dichroism of rhIL-1R(II). The near-UV circular dichroism (CD) was performed on a Jasco J-810 spectropolarimeter (Jasco Inc., Easton MD), using a 1 cm sample flow cell with temperature control. The sample was diluted to 1 mg/mL with sample buffer to achieve 2 mL for analysis. The protein concentrations were determined by A_{280} . Instrument control and data collection used Spectra Manager (Jasco Inc., Easton MD). The spectra were continuously scanned from 350 to 250 nm at a rate of 20 nm/min and 0.1 nm data pitch. The bandwidth for the scans was set at 1 nm with a response time of 4 s, and the sensitivity was set at 100 mdeg. The final scan for each run was comprised of nine averaged scans. The processed data were then converted to molar ellipticity, $[\theta]$ (see Figure 1).

Microcalorimetry of rhIL-1R(II). Urea solutions were freshly prepared for the DSC scans. All protein unfolding experiments were carried out using a calibrated vp-DSC instrument (MicroCal, LLC). Protein thermal reversibilities were carried out using a scan rate of 1 °C/min. For these experiments, a protein concentration of 0.44 ± 0.04 mg/mL in the presence and absence of 2 M urea (nondenaturing by CD at

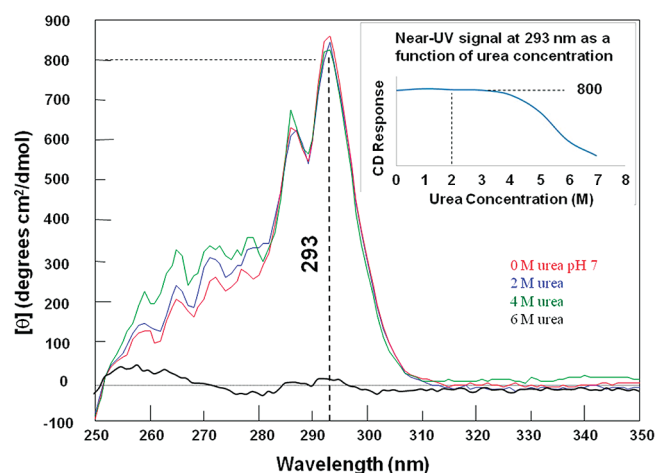


Figure 1. Near-UV CD data showing the extent of tertiary structure change of rhIL-1R (type II) as a consequence of urea concentration at pH 7 and 25 °C. The inset shows plotted changes of the CD response in units of molar ellipticity at 293 nm at designated urea concentrations. Note the protein retains native structure in 2 M urea.

25 °C, see Figure 1) was used, and 0.1 M sodium phosphate was included for buffer capacity at pH 7 during heating. Thermal reversibility was determined by dividing the enthalpy of the second consecutive scan by the enthalpy of the first scan reported as a percent.²⁹ The interval between scans was approximately 1 h. Microcalorimetric scan-rate-dependent studies were carried out with 2 mg/mL of rhIL-1R(II) in the PBS solution. The tested scan rates were 0.25, 0.5, 1.0, and 1.5 °C/min.³⁰ All data were evaluated using Origin software (version 7). Buffer–buffer baselines and progress baselines were subtracted in processing the DSC data. All thermograms presented were concentration normalized.

Study Conditions. In theory, different aspects of the thermodynamic process are at work below and above the T_m . The effect of urea to influence thermodynamic processes when the protein was predominantly unfolded required experimental attention on temperatures above the apparent T_m (or T_{app}). Furthermore, because the unfolded state was predominantly populated above the T_{app} , the ability to study the influence of urea to thwart unfolded protein interactions could be readily examined. For this reason, a temperature of approximately 70 °C (above the T_{app}) was chosen to study the properties of rhIL-1R(II).

Heating Experiments With and Without Urea. Two solutions, one with 2 M urea and the other without (control), were prepared in 0.1 M phosphate (pH 7) to examine the behavior of 2 mg/mL of rhIL-1R(II) heated at 70 °C (conditions where the protein was predominantly unfolded) for two minutes. The solutions were heated with a heating block as described previously³⁰ and then subjected to size exclusion chromatography to quantitatively assess aggregation.

Size Exclusion Chromatography. Size exclusion data from the heating experiment samples were helpful in determining the amount of aggregation, expressed as a percent of the total protein peaks as reported previously.³⁰ Analyses were carried out on a HP-1100 HPLC system. Samples were eluted off a TosoHaas TSK-G3000 SWXL column at a flow rate of 1 mL/min using an eluent consisting of 100 mM phosphate (pH 6.5) and 50 mM NaCl. Absorbance at 220 nm was measured for all eluting components. A 20 μ g injection load was used per HPLC run.

■ TOLUENE ENTROPY PROBE EXPERIMENTS

Free Energy from Equilibrium Solubility Measurements. The approach relied upon using a hydrophobic molecule as a probe to investigate thermodynamic properties in two different composite solvent environments. The first solvent studied was in aqueous 0.1 M sodium phosphate (abbreviated as “p”), and the second was in 2 M urea + 0.1 M sodium phosphate (abbreviated as “up”). Toluene was selected as the hydrophobic probe molecule for this study because it has a relatively low vapor pressure (similar to water) within the temperature regime of the study and also because it is less toxic than benzene. Transfer free energies were determined by transferring pure liquid toluene into either of the composite solvents. Toluene equilibrium solubility measurements in either composite solvent at designated temperatures were performed using the sealed-cuvette method of Smith et al.³¹ The transfer free energy of toluene to the final solution, ΔG_t^s (where the subscript “t” denotes toluene and the superscript “s” refers to either tp or tup solutions), can be calculated using eq 1

$$\Delta G_t^s = -RT \ln(n_t^s/n_t) \quad (1)$$

where R is the gas constant; T is temperature (K); n_t^s is the molar concentration of the toluene in the aqueous solution at equilibrium; and n_t is the pure toluene molar density.³²

The toluene absorbance standards were found to be stable for at least a month at room temperature sealed in 50 mL volumetric flasks. The sealed-cuvette method without stirring was used to determine equilibrium solubilities.³¹ Approximately 3 mL of phosphate solution was placed in a 3.5 cc, 10 mm light path, Hellma quartz cuvette (Cat#110-10-40), and a layer of 0.5 mL of toluene was added to the top of the urea solution, sealed with the accommodating Teflon cap, and placed in the UV-visible instrument (Spectra MAX Plus, Molecular Devices Corporation) with an electrically heated sample compartment (temperature control within ± 1 °C). Equilibrium concentrations were attained by repeated measurements at designated temperatures until no further change in absorbance was detected (extending out to several days to weeks in some cases), measured to within ± 0.01 mg/mL. Measurements were repeated to ensure the same concentration end point was attained for a given temperature.

Microcalorimetry. The DSC measurements for the following toluene solution studies were carried out in the vp-DSC assigning the composite solvent without toluene for the reference cell and toluene in the same composite solvent for the sample cell. The concentration of toluene in the sample cell was approximately close to that at the minimum temperature of equilibrium solubility within 10% error. The scan ran from approximately 20 to 40 °C and the raw data noted from the calorimeter in the vp-DSC were in units of calories/kelvin. Degradation of the urea during the time frame of the experiment was checked by pH measurement (with and without phosphate-buffered solutions) and found to be stable within the time frame of the scanned experiment and across five repeated scans. At least three replicate scans were averaged for a single experiment. The baseline repeatability of each scan was within the manufacturer's specifications (1.25 μ cal/°C).

The apparent heat capacity difference measurements for water and composite solvents (without toluene) were conducted with either water or composite solvents in both reference and sample cells. The scans were performed using the same scanning parameters as the toluene solution scans and

with the same number of replicates. These experiments were necessary to determine the parameters, $\Delta C_{p,w-c}$ and $\Delta C_{p,c-s}$ in eqs 3 and 4 described below. These parameters were obtained by determining the difference in the calorimetric heat capacities between composite solvents and water as well as the change between respective composite solvents and the corresponding toluene-containing solutions.

Density Measurements. The densities of the solutions were evaluated using a sensitive Anton Paar oscillating U-tube digital densimeter (DMA 5000). Measurements were stable to within the fifth and sixth decimal places. Test solutions were prepared as described below for both solution conditions (with and without urea) and with and without toluene. Densities were measured across the temperature range from 10 to 40 °C.

Equations for Change in Heat Capacity of Toluene in Composite Solvents. The apparent molar heat capacity of toluene in the two different composite solvents (subscript c) was compared: all else equal and allowing for temperature dependence, one solvent without urea and the other with 2 M urea (subscript u). The densities of the composite solvents ρ_c (with or without urea) and the densities of the final solutions with toluene (subscript s), ρ_s , were measured at various temperatures ranging from 5 to 40 °C as described above. The total mass concentration (grams) for a given component in the calorimeter cell is denoted by c followed by the corresponding subscript. MW is the molecular weight of a given component (defined by a given subscript).

To derive the apparent molar heat capacity of toluene in a composite solvent using calorimetric measurements, the molar heat capacity of the composite solvent, consisting of water (subscript w) and added ingredients (referred to as subscript a), Na_2HPO_3 (subscript p), Cl^- (subscript l; accounted for the ion when titrated to reach target pH with HCl), and urea, needed to be calculated. In the composite solvent without urea, the concentration of urea will be zero. In all the subsequent calculations, V_{cell} is the calorimetric cell volume (matching cell volumes for the vp-DSC used in these experiments was 0.50281 mL).

The molar heat capacity of the composite solvent can be derived from a separate set of calorimeter experiments as follows

$$C_{p,c} = (C_{p,a} \times N_a + C_{p,w} \times N_w) / (N_a + N_w) \quad (2)$$

where $C_{p,w}$ is the molar heat capacity of water obtained from the Steam Tables,³³ and $N_w = V_{\text{cell}} \times (\rho_c - c_u - c_p - c_l) / \text{MW}_w$ is the number of moles of water in the composite solvent. $N_a = V_{\text{cell}} \times (c_u / \text{MW}_u + c_p / \text{MW}_p + c_l / \text{MW}_l)$ is the total number of moles of added ingredients. For the case without urea, the urea contribution to N_a would necessarily be zero. The apparent molar heat capacity of the added ingredients can be calculated from the calorimeter data as follows

$$C_{p,a} = C_{p,w} \times v_a / v_w - \Delta C_{p,w-c} / N_a \quad (3)$$

where $v_a = (V_{\text{cell}} - V_w) / N_a$ is the apparent molar volume of the added ingredients and $V_w = V_{\text{cell}} \times (\rho_c - c_u - c_p - c_l) / \rho_w$ is the volume of the calorimeter cell occupied by water. $v_w = \text{MW}_w / \rho_w$ is the partial molar volume of water in the cell. The $\Delta C_{p,w-c} / N_a$ term refers to the calorimetrically measured excess molar heat capacity difference between the water (run in both reference and sample cells of the calorimeter) and a given composite solution (run in both reference and sample cells of

the calorimeter). Equations 3 and 4 are in the form of the expression derived by Makhatadze and Privalov.³⁴

Finally, we can calculate the apparent partial molar heat capacity of toluene in either of the composite solvents as follows

$$C_{p,t}^s = C_{p,c} \times v_t^s/v_c - \Delta C_{p,c-s}/N_t \quad (4)$$

where the apparent partial molar volume of toluene in the final solution is given by $v_t^s = (V_{\text{cell}} - V_c)/N_t$ and where $V_c = V_{\text{cell}}(\rho_s - c_t)/\rho_c$ is the volume of the composite solvent in the cell. The molar volume of either composite solvent is then given by

$$v_c = 1/(c_u/MW_u + c_p/MW_p + c_l/MW_l + (\rho_c - c_u - c_p - c_l/MW_w))$$

The number of moles of toluene in solution can be calculated by $N_t = c_t/MW_t$.

The change in the excess partial molar heat capacity of toluene can thus be calculated using eq 5.

$$\Delta C_{p,t}^s = C_{p,t}^s - C_{p,t} \quad (5)$$

The change in heat capacity is the difference between the partial molar heat capacity of toluene in either composite solution less the molar heat capacity of pure toluene at a corresponding temperature. The heat capacity for pure toluene as a function of temperature and the method adopted to perform the measurements calorimetrically have been described previously by Makhatadze and Privalov.³⁴

Enthalpy of Toluene in Aqueous Composite Solutions. The solution enthalpy can be determined if the change in heat capacity ($\Delta C_{p,t}^s$) is known (eq 5). An expression for the enthalpy, ΔH_t^s , as a function of the $\Delta C_{p,t}^s$ is shown in eq 6,³⁵ where T_h is the temperature of minimum solubility of toluene (K) and T is any reference temperature (K).

$$\Delta H_t^s = \int_{T_h}^T \Delta C_{p,t}^s dT \quad (6)$$

The approximate temperature of minimum solubility for toluene in the sodium phosphate solution was 18 ± 2.2 °C (291 K; solubility of 0.599 mg/mL), which is close to that in water.^{35,36} The minimum solubility was found to be approximately 3.5 ± 2.2 °C (276 K; solubility of 0.699 mg/mL) for toluene in 2 M urea + 0.1 M sodium phosphate based on our measurements.

Solvation Entropy. Knowing ΔH_t^s (eq 6) in either composite solution and corresponding ΔG_t^s (eq 1), it becomes possible to simply solve for ΔS_t^s by rearranging the familiar Gibbs–Helmholtz equation.

$$\Delta S_t^s = (\Delta G_t^s - \Delta H_t^s)/(-T) \quad (7)$$

Alternatively, it can also be calculated through $\Delta C_{p,t}^s$ as follows

$$\Delta S_t^s = \Delta S_t^s(T_h) + \int_{T_h}^T \Delta C_{p,t}^s d \ln T \quad (8)$$

where $-T\Delta S_t^s(T_h)$ is equal to $\Delta G_t^s(T_h)$. The two equations give similar results in the region where the density, calorimeter, and solubility data are available. They differ more in the extrapolated region. Below we present the extrapolated results using eq 8. Solvent entropies were determined as a function of temperature within the 20–40 °C temperature regime. For temperatures greater than 40 °C and up to 75 °C, extrapolated values were used to estimate entropies beyond the experimental

limits. To check the validity of our measurements with the literature for enthalpies of toluene in 2 M urea, it was found that there was approximate agreement with measurements made by Hovorka et al.,³⁷ although a temperature-dependent heat capacity for their results was not attainable.

RESULTS

Thermal unfolding of rhuIL-1R(II) was conducted using the microcalorimeter to study solution conditions at an optimal pH where the T_{app} was at a maximum (\sim pH 7). The initial calorimetric studies were performed with the protein concentration at 0.44 mg/mL (or 0.0115 mM). At this concentration, protein aggregation was inhibited during the calorimetric heating experiments and found to be partially reversible. Although the addition of 2 M urea shifted the transition maximum to low temperature, significant improvement in thermal reversibility was found from 46% in its absence to 91% in its presence (Figure 2). The dramatic increase in reversibility when urea was present was of particular interest since it suggested some resistance to unfolding-mediated aggregation.

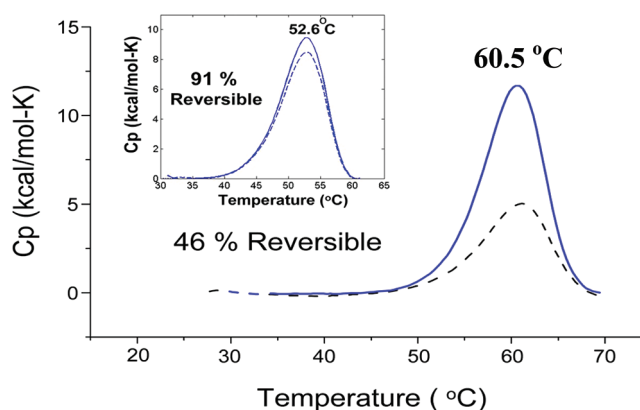


Figure 2. Thermal reversibility data for rhuIL-1R(II) at 0.44 mg/mL in 0.1 M sodium phosphate (pH 7) without 2 M urea and with 2 M urea (inlay). Dashed traces in both cases shown are the second consecutive scans. Reversibilities in each case are shown as a percent.

To examine the properties of the unfolding transition in the presence and absence of urea, a scan-rate dependent model³⁰ was applied to deconvolute the unfolding transition into two components (Figure 3). A low temperature component was associated with the enthalpy of protein unfolding (ΔH_{unf}) and a higher temperature unknown component with endothermic heat (ΔH_{unk}) depicted in Figure 3A and B. Justification for this was suggested by a $\Delta H_{\text{cal}}/\Delta H_v$ ratio of 0.8 for the case without urea and 0.9 in its presence (accepting that the greater irreversibility of the former could impose more error in the quantification of calorimetric to van't Hoff ratio). The determination of ΔH_v is based upon the calculation of Privalov et al.³⁸ In the absence of urea (Figure 3A), the ΔH_{unf} was approximately 81 kcal/mol, while the ΔH_{unk} was found to be 18 kcal/mol ($\Delta H_{\text{cal}} = 99$ kcal/mol). Furthermore, a ΔH_{unf} of 82 kcal/mol was obtained from optimal fits for this solution case. The fit for the case without urea is based upon our previous work³⁰ with the following simplifications and assumptions. The aggregation pathway was modeled by the second-order term only. The thermodynamic parameters T_m and ΔH_m are assumed to be the same as in the 2 mg/mL case. For the

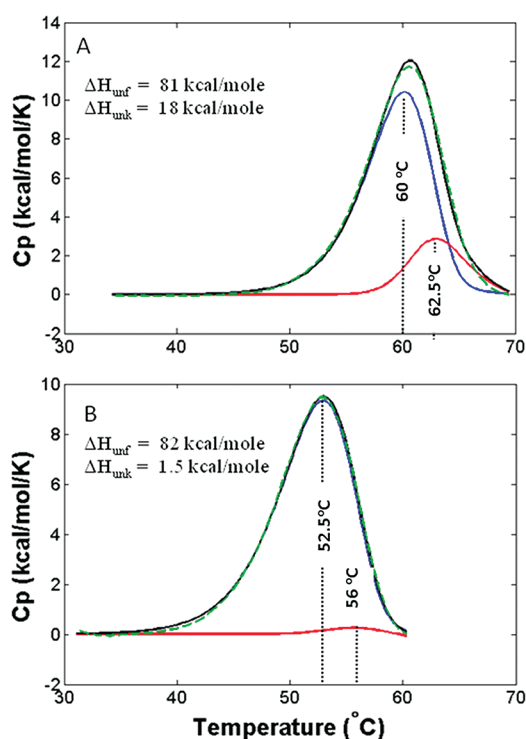


Figure 3. Deconvolution of initial scans of rhuIL-1R(II) at 0.44 mg/mL in 0.1 M sodium phosphate (pH 7) without 2 M urea (A) and with 2 M urea (B). The low temperature unfolding transition in each case (blue) originates from the N→U unfolding, and the endothermic contribution of the high temperature transition (red) is unknown excess endothermic heat. Enthalpy values of unfolding (ΔH_{unf}) and unknown (ΔH_{unk}) origin are displayed. The complete transition envelope depicts the fitted (black) or sum of the deconvoluted peaks using the simulation model (ref 30), and the experimentally measured transition is shown by the dashed contour.

case with urea, there are alternative ways to deconvolute the apparent calorimetric heat without further constraint from additional knowledge. The case presented in Figure 3B is fitted with the assumption that the T_m is shifted to lower temperature by the same amount as the shift in T_{app} .

Since the case with urea is about 91% reversible (Figure 2), it is assumed to approximate a virtually reversible system. Thus, ascribing the protein unfolding to be approximately constant in the unfolding temperature regime with and without urea seemed reasonable based upon the associated error of the fitted data. Thus, in the case with urea (Figure 3B), the ΔH_{unf} remained the same, while the ΔH_{unk} was about 3-fold lower at 1.5 kcal/mol ($\Delta H_{\text{cal}} = 83$ kcal/mol), ascribing to the additional excess heat above the unfolding transition and a small contribution to the irreversibility.

To examine if the thermal transition was kinetically controlled, a microcalorimetric scan-rate experiment was conducted at 2 mg/mL in the absence of urea. The results are shown in Figure 4 and depict shifts to high temperature concomitant with increasing scan rates from 0.25 to 1.50 °C/min. This behavior is consistent with an irreversible degradation pathway that is kinetically controlled.^{39,40} The low temperature deconvoluted transition enthalpy related to the unfolding of the protein did not seem to change, while the high temperature transition exhibited an excess heat of approximately 50 kcal/mol in comparison to that observed in the case without urea at 0.44 mg/mL. The results of the excess

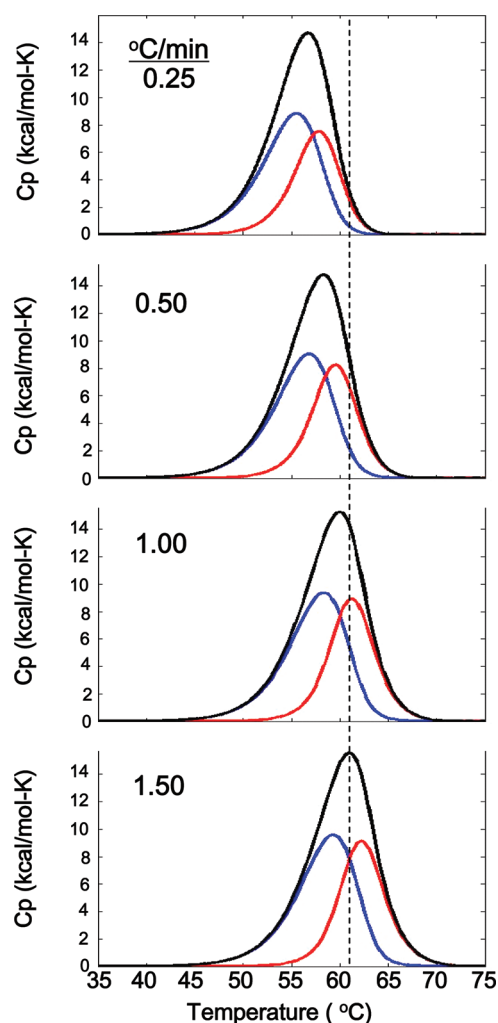


Figure 4. Scan-rate-dependent unfolding transitions of rhuIL-1R(II) at 2 mg/mL in PBS showing deconvoluted enthalpies assigned to unfolding (blue) and unknown excess heat (red). Scan rates are displayed in each case. The data shown are deconvolutions of scan-rate data using the deconvolution modeling routine described in ref 30. The vertical dashed line is a reference to examine scan-rate-dependent shifts in transition temperatures. Note that the high transition unknown endothermic peak exhibits scan-rate dependence.

enthalpic heat attributed to ΔH_{unk} for the cases studied appeared to correlate with the irreversible nature of the unfolding process within the calorimeter time scale and are presented in Table 1. Specifically, the greater the thermal irreversibility, the greater the ΔH_{unk} contribution in the unfolding transition envelope.

The role of urea to increase thermal reversibility was cause to see if there might be a correlation with its ability to inhibit aggregation.²¹ Therefore, heating experiments above the T_{app} at 70 °C where the protein was predominantly unfolded in the presence and absence of 2 M urea (all other solution factors being equal) were investigated. The soluble aggregates were

Table 1. Parameters of Thermal Irreversibility and ΔH_{unk}

sample	irreversibility (%)	ΔH_{unk} (kcal/mol)
w urea @ 0.44 mg/mL	9 ± 2	1.5 ± 2
w/o urea @ 0.44 mg/mL	54 ± 3	18 ± 3
w/o urea @ 2 mg/mL	80 ± 6	50 ± 5

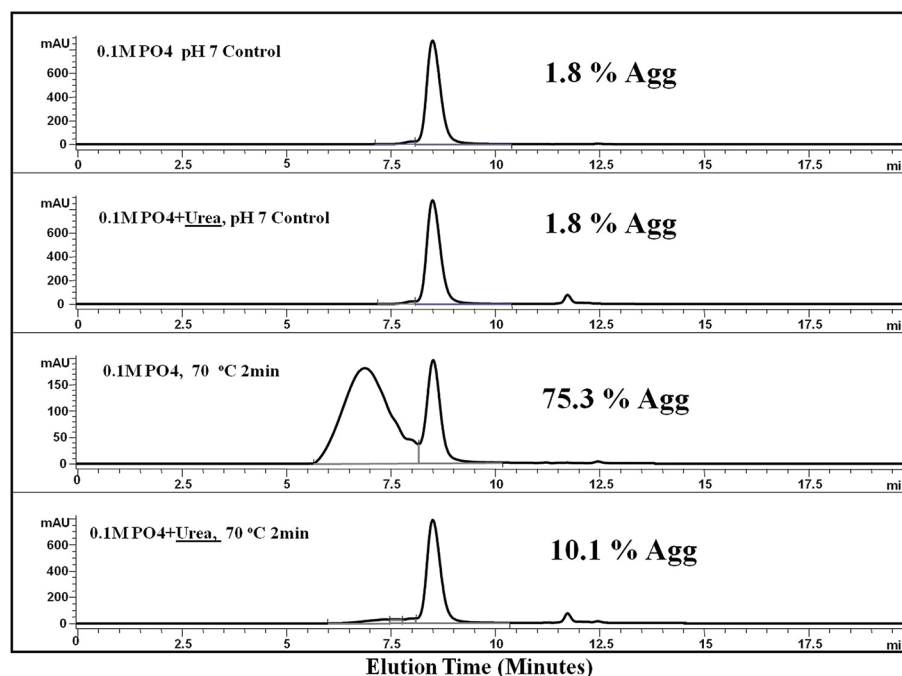


Figure 5. Size-exclusion chromatographic data showing the effects of 2 M urea on aggregation for solutions containing 2 mg/mL rhuIL-1R(II) at 70 °C heated for approximately 2 min. Solution conditions are displayed and consist of 0.1 M sodium phosphate (pH 7) with and without urea.

measured using SEC after being heated for 2 min at a concentration of 2 mg/mL. Results of the study are shown in Figure 5. Apparent from the data is a striking contrast between the propensity to form aggregates when urea was present in the sample and the condition of its absence. Indeed, incorporation of 2 M urea in the sample exhibited a prominent resistance to form soluble aggregates (from 1.8% to 10.1%) and correlated with the high thermal reversibility observed in the microcalorimetry experiments (Figure 2). Moreover, in the absence of urea, the aggregation of the sample increased from 1.8% to 75.3%, consistent with the rates already presented previously where massive aggregation was observed in kinetic experiments near this temperature.³⁰

To try and answer the question as to why urea had such a pronounced impact on inhibiting aggregation when the protein was primarily in an unfolded state, the same solution was examined using toluene as a hydrophobic probe to ascertain its thermodynamic properties. It has been reported in the literature that urea-containing solutions can increase (e.g., less negative than in pure water) solvation entropy of hydrophobic molecules.¹³ The low solubility of hydrophobic compounds in water is a manifestation of the negative entropy of solvation which overcomes a favorable enthalpy of solvation. Equilibrium solubility experiments in 0.1 M sodium phosphate without and with urea are shown in Figure 6, depicting a shift in the temperature of minimum solubility from approximately 18 °C to ~3.5 °C, respectively. In addition to this observation, there was a clear increase in equilibrium solubility for toluene when urea was added to the solution as expected. The thermodynamic parameters for toluene in the composite solution without urea are shown in Table 2, and those containing urea are shown in Table 3.

From the results listed in Table 4, the data suggest a relative decrease in the change in solvation free energy in the 2 M urea composite solution to be approximately 20% relative to the same without urea up to 50 °C. Upon further heating to 75 °C,

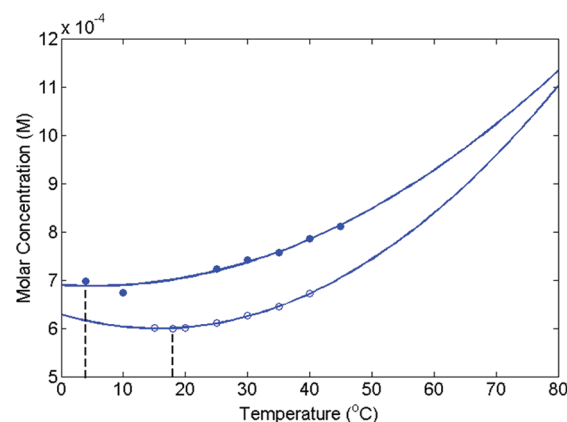


Figure 6. Solubility data for toluene in 2 M urea + 0.1 M sodium phosphate (filled ovals) and in 0.1 M sodium phosphate (unfilled ovals). Solubility is expressed in terms of molarity of toluene in either phase. Vertical dashed lines exhibit approximate temperatures of minimum solubility in each case.

the change in solvation free energy narrows to a 7% decrease in comparison to the solution without urea (Figure 7A). This would suggest the entropic component of the free energy is dominant up to 75 °C accounting for the negative sign to the free energy (Figure 7B). Moreover, a decrease in the entropic driving force translates into less negative solvation entropy in the case with urea (comparing $T\Delta S$ values in Tables 2 and 3). Apparent from Table 4, the $\Delta\Delta G_t^{\text{up-tp}}$ is negative in sign and therefore spontaneously solvates toluene more readily in the urea containing solution than in the same without. Note that the $\Delta\Delta H_t^{\text{up-tp}}$ values are all positive, and thus the entropy term is responsible for the negative free energy and therefore the driving force for the increased solvation in the urea containing solution. This appears to be true across the entire unfolding transition range although to a lesser extent at temperatures above 50 °C (323 K).

Table 2. Thermodynamic Parameters of Toluene Solubility in 0.1 M Sodium Phosphate^a

temperature (K)	$n_t^{s=tp}$ (M)	$\Delta G_t^{s=tp}$ (cal/mol)	$\Delta H_t^{s=tp}$ (cal/mol)	$\Delta C_{p,t}^{s=tp}$ (cal/(mol K))	$T\Delta S_t^{s=tp}$ (cal/mol)
288	6.010×10^{-4}	4170	−231	77.8	−4401
291	5.990×10^{-4}	4210	0	76.2	−4210
293	6.010×10^{-4}	4236	151	75.2	−4085
295	(6.020×10^{-4})	(4262)	(301)	(74.1)	(−3961)
298	6.110×10^{-4}	4297	521	72.6	−3776
303	6.260×10^{-4}	4352	877	70.0	−3475
308	6.450×10^{-4}	4401	1221	67.5	−3179
313	6.720×10^{-4}	4443	1553	65.0	−2891
318	(7.048×10^{-4})	(4481)	(1872)	(62.7)	(−2609)
323	(7.435×10^{-4})	(4513)	(2180)	(60.4)	(−2334)
333	(8.391×10^{-4})	(4565)	(2761)	(56.0)	(−1804)
343	(9.589×10^{-4})	(4603)	(3300)	(51.8)	(−1304)
348	(10.279×10^{-4})	(4618)	(3554)	(49.9)	(−1064)
SD =		±18	±337	±5.5	±390

^aValues in parentheses are estimates based on a linear fit to molar volume data and are either interpolated or extrapolated where insufficient data were available. The superscript for s=tp refers to the solution of toluene in 0.1 M sodium phosphate.

Table 3. Thermodynamic Parameters of Toluene Solubility in 2 M Urea + 0.1 M Sodium Phosphate^a

temperature (K)	$n_t^{s=tp}$ (M)	$\Delta G_t^{s=tp}$ (cal/mol)	$\Delta H_t^{s=tp}$ (cal/mol)	$\Delta C_{p,t}^{s=tp}$ (cal/(mol K))	$T\Delta S_t^{s=tp}$ (cal/mol)
277	6.980×10^{-4}	3941	29.6	59.1	−3911
283	6.740×10^{-4}	4021	383	58.4	−3639
288	(6.958×10^{-4})	(4084)	(674)	(57.8)	(−3411)
291	(7.012×10^{-4})	(4121)	(847)	(57.4)	(−3275)
293	(7.056×10^{-4})	(4144)	(962)	(57.1)	(−3184)
295	(7.107×10^{-4})	(4167)	(1076)	(56.8)	(−3093)
298	7.195×10^{-4}	4200	1245	56.3	−2956
303	7.374×10^{-4}	4252	1525	55.6	−2729
308	7.592×10^{-4}	4301	1801	54.8	−2502
313	7.851×10^{-4}	4347	2072	53.9	−2276
318	8.149×10^{-4}	4389	2340	53.1	−2051
323	(8.487×10^{-4})	(4428)	(2603)	(52.2)	(−1827)
333	(9.283×10^{-4})	(4498)	(3116)	(50.4)	(−1383)
343	(10.238×10^{-4})	(4559)	(3612)	(48.6)	(−948)
348	(10.775×10^{-4})	(4586)	(3853)	(47.7)	(−734)
SD =		±18	±290	±5.1	±330

^aValues in parentheses are estimates based on extrapolation. The superscript for s=tp refers to the solution of toluene in 2 M urea + 0.1 M sodium phosphate.

Table 4. Thermodynamic Parameters for Toluene in 0.1 M Sodium Phosphate and 2 M urea + 0.1 M Phosphate Solutions

temperature (K)	$-T\Delta\Delta S_t^{sup-tp}$ (cal/mol)	$\Delta\Delta H_t^{sup-tp}$ (cal/mol)	$\Delta\Delta G_t^{sup-tp}$ (cal/mol)	$\Delta\Delta G_t^{sup-tp}/\Delta G_t^{tp}$
288	−991	906	−85	−20.4%
291	−937	847	−90	−21.3%
293	−903	810	−92	−21.8%
295	−870	775	−95	−22.2%
298	−822	724	−97	−22.7%
303	−747	648	−100	−22.9%
308	−679	579	−99	−22.6%
313	−616	520	−97	−21.8%
318	−560	468	−92	−20.5%
323	−508	423	−85	−18.8%
333	−422	356	−67	−14.6%
343	−357	312	−45	−9.7%
348	−331	299	−32	−7.0%

DISCUSSION

Evidence for an Entropically Driven Aggregation Mechanism. The identity of the endotherm feature pertaining to the high temperature side of the transition envelope, ΔH_{unk} (Figure 3), is consistent with the endothermic heat generated by an entropically driven reaction.^{41–43} Evidence that this component of the unfolding envelope is associated with aggregation was manifested by the $\Delta H_{cal}/\Delta H_v$ ratio being less than 1 and consistent with intermolecular interactions that distort the transition by irreversible aggregation effects.⁴⁴ The endotherm occurs in a temperature region where massive aggregation has been characterized for rhuIL-1R(II).³⁰ It succeeds the protein unfolding event, consistent with unfolding as a prerequisite for the aggregation phenomena. Furthermore, there was no evidence for any exothermic heat where massive aggregation was known to occur in this temperature region. The scan-rate dependence was consistent with a kinetically controlled process (Figure 4). The fact that both transitions showed scan-rate dependence suggests that the unfolding and aggregation events are both related. Since there was no other evidence for another competing reaction, the aggregation

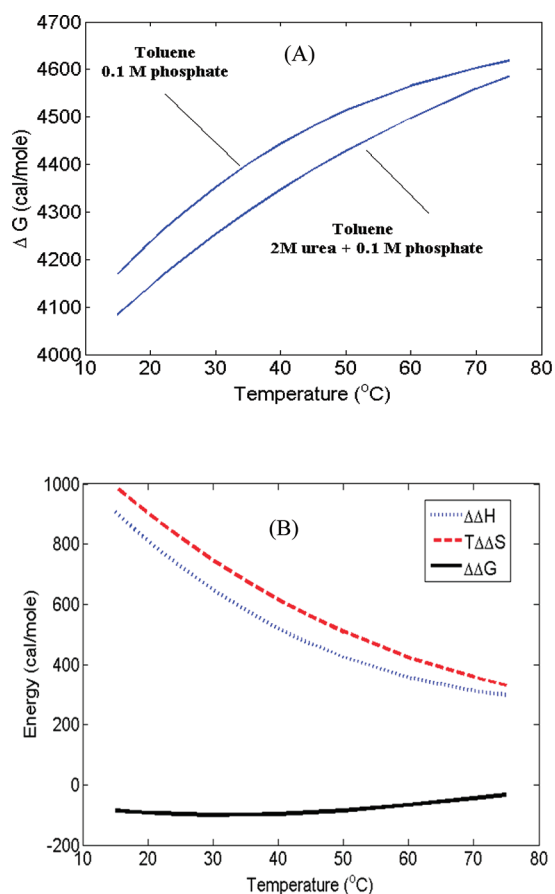


Figure 7. Change in solvation free energy as a function of temperature with respect to toluene transfer into solutions with and without 2 M urea (A). A comparison of the $\Delta\Delta H$ and $T\Delta\Delta S$ solvation responses to the $\Delta\Delta G$ (B). Note that the entropy component of the free energy difference dominates.

pathway appeared likely the cause of the scan-rate behavior. Thermal irreversibility tended to directly correlate with ΔH_{unk} (Table 1). Taken together, these findings would suggest that the deconvoluted high temperature endothermic heat of the transition envelope is best aligned with an entropically driven aggregation process where the unfolded exposed hydrophobic surface becomes displaced from the hydrophilic solvent by means of aggregation.

Another possibility for the increased endothermic heat could be from additional unfolding of the protein or perhaps from a populated stable intermediate. If the protein showed increased unfolding in the concentration normalized thermogram, this should likely be independent of concentration influence where the T_{app} is essentially the same. Examination of DSC scans in the absence of urea at 2 mg/mL (Figure 3A) with that at 0.44 mg/mL (Figure 2) clearly showed that although the T_{app} values are similar there is additional heat in the 2 mg/mL sample (Table 1, Figure 4). Moreover, there was no evidence that an intermediate state of unfolding was present since the $\Delta H_{\text{cal}}/\Delta H_{\text{v}}$ ratio in that case would necessarily need to be greater than 1. This evidence argues against additional heat by a populated intermediate state and increased unfolding with increased temperature within the error of our measurements.

If the thermal irreversibility correlated with ΔH_{unk} and aggregation, then the converse must also be true, that greater thermal reversibility is correlative with conditions where

aggregate proneness is reduced. This seemed to be the case when urea was added to the solution environment since there was a significant increase in thermal reversibility (Figure 2). The idea was further tested by the heating experiment in the phosphate solution with and without urea. As depicted in Figure 5, there was a remarkable reduction in propensity to form aggregates at conditions where the majority of the protein was in the unfolded state (well above the T_{app}). These findings seemed to corroborate the idea that the increased thermal reversibility in the presence of urea was a signature for the reduced tendency of the unfolded protein to aggregate. This is perhaps not surprising given that conditions that would increase thermal reversibility have been previously shown to correlate with a lower tendency to aggregate in other protein systems.²⁹

Evidence for Greater Entropy in Urea Solutions.

Although the toluene probe experiments were not a perfect representation of the urea solution properties in the presence of rhuIL-1R(II), they do provide some insight concerning the impact of urea in the solvent that affects the thermodynamic properties for hydrophobic intermolecular reactions at elevated temperatures. The solvation entropy of the toluene containing solution does increase as expected in the presence of urea.¹³ The entropy increase would likely reduce the hydrophobic driving force that would cause unfolded surfaces to interact by approximately 20% up to 50 °C (323 K). This difference between the two solutions diminishes with heating up to 75 °C or 348 K (Table 4).

Proposed Mechanism. The lingering question to be answered concerning the influence of urea at low (subdenaturing) concentrations in aqueous solution is whether it interacts more strongly with the solvent or with the protein. There has been evidence gathered for the direct binding interaction of urea with proteins or peptides even at relatively low concentrations like those used in our experiments.^{45,46} There has been reported evidence using pair correlation functions to show the preference of urea to hydrogen bond with backbone amide groups more so than water.^{47,48} Such interactions are expected to be weak at low urea concentrations.¹⁹ Urea has been reported to displace water around the protein without substantially disturbing the solution structure and the local density around the protein.⁹ Urea has been reported to preferentially solvate polar (asparagine, glutamine, histidine) and nonpolar (leucine, isoleucine, methionine, phenylalanine) residues with a displacement ratio of five molecules of water for every two urea molecules that bind.⁴⁶ Solvation of nonpolar groups in urea has been described as an entropic phenomenon.¹⁷ In this process hydrophobic interactions are believed to be weakened.⁴⁹

How urea affects water structure has been the subject of debate concerning whether or not water structure is altered.^{14,15,50} More recent neutron diffraction evidence suggests that urea incorporates readily into water, forming hydrogen bonds with water through both its amines and carbonyl headgroup as well as to itself forming urea chains.¹⁶ Furthermore, neutron diffraction studies have suggested that at a urea to water mole ratio of 0.25 both urea and water do not appreciably segregate but that water in the first hydration shell of urea is radically modified in comparison to bulk water. Thus, water structure appears to be altered to some extent where it interacts with urea. Probing further, it has been pointed out that hydrogen bonds between water molecules around urea's amine groups are like those found for water molecules around

nonpolar groups with the greatest alterations in hydrogen bond angles.⁵¹

The idea that the entropy of water would be reduced in the presence of the protein hydrophobic surface is made more credible from X-ray diffraction evidence of crambin crystals showing ordered water structure surrounding hydrophobic protein surfaces.⁵² Evidence that exposure of such surfaces in aqueous phases could potentially form such orderly solvent structural arrangements accompanied by an unfavorable solvation entropy contribution has been a premise to explain the hydrophobic effect.⁵³ Such hydrophobic exposure can drive protein–protein aggregation.^{54–58} Hydrophobic interactions of this kind have been envisaged as entropically driven mediated by the displacement of clathrate-like water from the hydrophobic surface.⁵⁹ This also would be consistent with the aggregation mechanism of rhuIL-1R(II). Yet, these clathrate-like water assemblages have not been considered as rigid orderly structures in the solution phase, and this idea has been challenged regarding the geometrically implausible nature of such structures where the hydrophobic surface is expansive as might be found when protein greatly unfolds or aggregates.⁵⁸ However, in the case where a molten globular-like structure exhibits a partially unfolded or exposes clusters of hydrophobic surface that are not expansive, these clathrate-like water structures could likely be possible (though transient) and contribute to a lowering of solvation entropy. An explanation for the unfavorable enthalpy and favorable entropy of transferring nonpolar solutes from water to urea solution has been described as a decrease in the hydrophobic effect arising from the displacement of some water molecules in the solvation hydration shell by urea.¹⁷ It is suggested that this behavior with urea should also be true for proteins that unfold and preferentially interact with urea, providing a barrier that opposes orderly water structure in contact with the bare hydrophobic surface. The preferential binding of urea to hydrophobic surfaces has been shown to weaken hydrophobic interactions.⁶⁰ Thus, by binding to the protein through hydrogen bonds, urea provides an enthalpically favorable interaction with the protein, while enabling an entropically favorable interaction with surrounding water. This idea would be in alignment with the diminished propensity of unfolded rhuIL-1R(II) to form aggregates.

Urea has been shown to increase the entropy of water structure around hydrophobic surfaces. For example, the number of hydrogen bonds per water decreased when 1 M urea was part of a solution with dialanine peptide.¹⁷ The reduction in hydrogen bonds was consistent with an increase in both entropy and enthalpy changes, causing the water around the methyl groups to be less ordered, consistent with an increase in ΔS . This behavior is certainly consistent with the toluene probe experiments where both entropy and enthalpy were shown to increase when urea was added to the solution (Tables 2, 3, and 4).

Solvation free energies have been assumed to be proportional to the solvent-accessible surface area of a particular group or amino acid residue.⁶¹ Toluene has about 275 Å² of hydrophobic surface per molecule.⁶² Knowing the surface area and concentration, it is possible to calculate the solvated hydrophobic surface area difference between the two solution environments based on toluene solubility. At 70 °C, for example, the extrapolated toluene solubilities without and with urea are 9.589×10^{-4} and 10.238×10^{-4} g/mL, respectively. The additional solvated hydrophobic surface can be calculated

to be 1.17×10^{20} Å²/mL. This is the approximate solvation benefit for the hydration of the hydrophobic surface due to the increased entropy when 2 M urea is in solution.

The folded native state of rhuIL-1R(II) has about 3979 Å² of hydrophobic surface (Molecular Operating Environment, MOE, used to calculate hydrophobic surface for I, L, V, M, F, W, and C residues). Assuming that this is the starting point in either solution well below the unfolding transition, if one were to consider the complete unfolding of rhuIL-1R(II) to a random coil or extended state, based on sequence this would amount to approximately 15 242 Å² of hydrophobic surface per molecule. Subtracting the native exposed hydrophobic surface area from the fully unfolded surface area, the additional surface to be solvated would be 11 263 Å² per molecule at 2 mg/mL.

To explain the inhibition exhibited in Figure 5 at 70 °C where the protein is predominantly in an unfolded state, if it is assumed that complete unfolding is attained, the difference in increased hydrophobic surface area solvated in the presence of urea for the remaining monomer in solution after 2 min would be approximately 2.33×10^{20} Å²/mL. This is about a 2-fold higher solvation capacity than the estimated solvation capacity for the hydrophobic surface based on the toluene solubility in the 2 M urea solution or 1.17×10^{20} Å²/mL. The result would suggest that unfolding of the molecule to expose half of its hydrophobic surface could be adequately sustained in the 2 M urea solution. It is reasonable if the protein does not unfold completely but partially. Moreover, the aggregation process itself will remove the unfolded exposed hydrophobic surface, further reducing the hydrophobic unfolded surface area from the aqueous solvent even though to a much less extent in the urea containing solution. The increased solvation entropy caused by urea would be expected to weaken the hydrophobic effect.

Is the increased entropy with 2 M urea sufficient to explain the reduced aggregation tendency at 70 °C (Figure 5)? To answer this question, it is important to note that there is a kinetic component to this reaction scheme and also an unknown equating of the increased change in entropy to the change in the hydrophobic driving force. The contributions from entropy slightly eclipse the enthalpy, although both are diminished to a great extent at this temperature (Table 4). Therefore, both can be considered contributors. Entropy certainly does play a role at these conditions and is increased so that it must reduce the hydrophobic effect to some degree, but enthalpy also is a factor. This is further supported by the associated $\Delta\Delta C_{p,t}^{\text{up}-\text{tp}}$ value of -5.6 cal/(mol K) at 70 °C, in agreement with a weakened hydrophobic effect. It is interesting to point out here that the absolute value of this change is on the order of the solvation heat capacity difference for urea (5 ± 1 cal/(mol K)) in water at 25 °C.⁵¹ Since the ΔC_p is a common thermodynamic parameter of the enthalpy and entropy terms of the Gibbs–Helmholtz equation, it is a useful parameter to confirm the diminished hydrophobic effect. Evidence for enthalpic contributions of urea to reduce the hydrophobic effect has been previously reported.⁶⁰

We acknowledge here that making assessments purely on the transfer of one type of hydrophobic molecule (i.e., toluene) to approximate the hydrophobic influence of all hydrophobic surfaces including different types of hydrophobic molecules is at best an approximate depiction. Different hydrophobic molecules do not ascribe their influence purely by exposure of surface alone and thus require some scaling factor to be applied to account for other aspects of influence unique to their

given hydrophobicities (e.g., structure, aromatic vs non-aromatic, saturated vs unsaturated, etc.). Our experiment just illustrates that the presence of 2 M urea in solution reduces the hydrophobic force that would drive rhuIL-1R(II) aggregation and is accompanied by an increased solvation entropy in the process.

As a further check, the approximate effect of the increase in entropy on the T_m shift associated with 2 M urea was estimated. At the T_m , the free energy is zero, and so $\Delta H_m - T_m \Delta S_m = 0$. Taking the differential, and solving for ΔT_m

$$\Delta T_m = \frac{\Delta \Delta H_m - T_m \Delta \Delta S_m}{\Delta S_m} \quad (9)$$

It can be shown that $\Delta S_m = \Delta H_m / T_m$. From the data published using our model, the $\Delta H_m = 74.3$ kcal/mol and the $T_m = 326.6$ K,³⁰ we get $\Delta S_m = 227.5$ cal/(mol K). Assuming the effect of urea on the protein in the solution is predominantly directed toward the hydrophobic surface, we can use the result from the toluene transfer data in Tables 2 and 3 as an approximation to estimate the entropy and enthalpy terms for protein unfolding. The entropy change can thus be calculated to be $\Delta \Delta S_t \sim 1.5$ cal/(mol K), and that for $\Delta \Delta H_t \sim 400$ cal/mol. For the ΔH_m and ΔS_m terms, it is assumed that the changes for both the native and the unfolded states are proportional to the accessible hydrophobic surface area (AHSA) and that the proportionality constant is approximately the same as for toluene. Then at 325.15 K, $\Delta \Delta H_m / \text{AHSA} = 400/275$ cal/mol/Å² and $\Delta \Delta S_m / \text{AHSA} = 1.5/275$ cal/(mol K)/Å². Since from the isothermal experiment described in Figure 5 the unfolding could progress to approximately half of the fully extended (or random coil) form, then to a first approximation there would be 11 263/2 Å² per molecule of hydrophobic surface or 5632 Å². Thus, $\Delta \Delta H_m = 8192$ cal/mol, and $\Delta \Delta S_m = 30.7$ cal/(mol K). Substituting these values into eq 9, we get $\Delta T_m = -8$ K or about an 8 °C shift to lower temperature. This suggests that the affect of the entropy increase with urea in the region of the unfolding temperature can make it easier for the protein to unfold by reducing the hydrophobic effect. This would translate to a lower unfolding temperature. The estimated T_m shift made using eq 9 seems to provide good agreement with experiment (Figures 2 and 3) and protein-unfolded hydrophobic surface area, where toluene, in this case, serves as a reasonable probe of the thermodynamic properties of solvation.

Consider what happens in the calorimeter as the temperature of the solution increases (Figure 8): the destabilizing effect of protein conformational entropy increases.¹³ This might occur as solvation entropy increases (becomes less negative) and thus weakens the hydrophobic core residue structure. The expected outcome would be accompanied by a lowering of the T_m as was the case in the 2 M urea + 0.1 M phosphate solution. Although somewhat weaker than at low temperature (Figure 7), there still is a dominant entropic component at work within the region of the unfolding transition (50–70 °C). This is most apparent from the $-T\Delta \Delta S$ term and its comparability to the $\Delta \Delta H$ term at 343 K (Table 4). The free energy decreases from ~19% to 10% in this temperature region in the presence of urea. Once the protein is unfolded, it is proposed that urea would likely interact with the peptide backbone and hydrophobic residues more intimately than in the bulk solution phase as depicted by a zone of entropic enhancement in Figure 8 (exaggerated in the cartoon for illustration purposes). This would be in alignment with the understanding that urea binds more to the unfolded

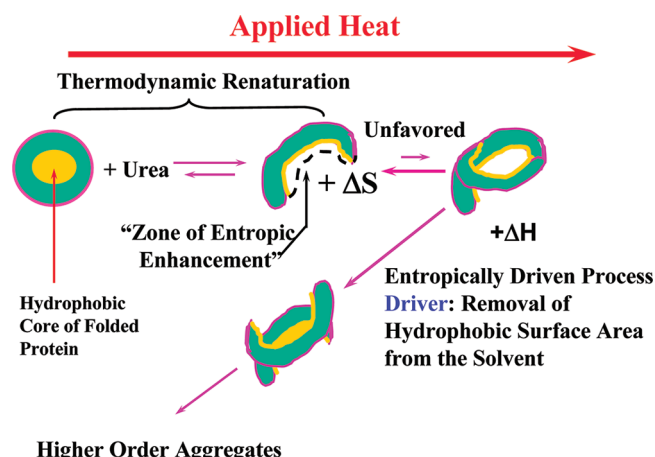


Figure 8. Schematic representation of the protein solution with urea and events during heating that are proposed to explain the high thermal reversibility and low susceptibility toward aggregation. A “zone of entropic enhancement” is described that is postulated to lower the entropic force that would normally cause the unfolded protein to form a complex, making the aggregation pathway less favorable.

state than to the native state^{46,63} and assumes a preference to bind to the nonpolar surface.¹² Although we suspect this to occur, due to the low urea concentration and elevated temperature of the unfolding transition for rhuIL-1R(II), the interactions with the protein exposed hydrophobic surface would likely be weak so that refolding or hydrophobic collapse in the thermodynamic renaturation process would still be possible but impeded due to a diminished hydrophobic effect.⁶⁴

It is difficult to ascertain whether the small shift of ~8 °C to low temperature (Figure 2) was facilitated by the denaturing interactions of urea directly with the protein or as an indirect consequence of weakened entropic influences in the solvent during heating. Moreover, it is not known to what extent the protein has unfolded in the heating process. Nonetheless, it is clear that at relatively low urea concentrations as those used in this study the solvation entropy dominates and becomes less negative with increased temperature, thereby reducing the hydrophobic interactions that would give rise to aggregates more so than when urea is not present in the solution. Furthermore, the findings of this study may provide some support for urea to stabilize a molten globular-like state as others have previously reported.^{5,6} Knowing that the interactions between urea and protein are already weak at low temperature (nondenaturing) and that there is an approximate 20% solvation free energy decrease attributed to a dominating solvation entropy contribution and an accompanying weakened hydrophobic effect at elevated temperature, it is hard to reconcile with another explanation for the observed findings provided by the 2 min heating experiment at 70 °C (Figure 5). The experimental evidence suggests a role for urea to reduce the hydrophobic effect with increased temperature, thus permitting unfolding at a lower temperature, and once unfolded, the entropy at the interface between the exposed hydrophobic surface of the protein and solvent is less negative to an extent that reduces unfolded-mediated aggregation of rhuIL-1R(II) that has been shown to be an entropically driven process.

CONCLUSIONS

The evidence presented conforms to a thermal unfolding rhuIL-1R(II) aggregation process that is entropically driven in the region of the T_m . The presence of 2 M urea has been shown to dramatically impede the process of aggregation and results in greater thermal reversibility. The destabilization of the transition as noted by a shift to low temperature when urea is present may be consistent with the stabilization of a molten-globular-like state for this molecule due to an overall reduction of the hydrophobic effect upon heating the solution. The role of urea to manipulate the entropy at the interface between the unfolded protein and the solvent is significant. The data presented align with the idea that urea acts to increase the solvation entropy of the exposed hydrophobic surface, thereby reducing the driving force that would otherwise promote the unfolded protein to more readily aggregate. The proposed macroscopic mechanism can explain how an entropically driven aggregation reaction is inhibited by urea at low concentrations for the case of thermally denatured rhuIL-1R(II).

AUTHOR INFORMATION

Corresponding Author

*Fax: 805-375-8519. E-mail: jianz@amgen.com.

Notes

The authors declare no competing financial interest.

ACKNOWLEDGMENTS

We would like to thank Professor George Makhatadze for helpful advice and constructive discussions concerning the thermodynamics of toluene/solution transfer and DSC experiments. We also thank Dr. Randal Ketchum for his surface area analysis of folded and unfolded rhuIL-1R(II). In addition, we thank Mary Wallace for her kind efforts in assisting with the acquisition of the scan-rate-dependent unfolding data along with operation of the vp-DSC. We would also like to thank MicroCal (GE healthcare) for their technical support.

REFERENCES

- (1) Schein, C. H. *Biotechnology* **1990**, *8*, 308–317.
- (2) Arakawa, T.; Timasheff, S. N. *Biochemistry* **1982**, *21*, 6536–6544.
- (3) Timasheff, S. N. *Annu. Rev. Biophys. Biomol. Struct.* **1993**, *22*, 67–97.
- (4) Volkin, D. B.; Verticelli, A. M.; Bruner, M. W.; Marfa, K. E.; Tsai, P. K.; Sardana, M. K.; Middaugh, C. R. *J. Pharm. Sci.* **1995**, *84*, 7–11.
- (5) Edwin, F.; Sharma, Y. V.; Jagannadham, M. V. *Biochem. Biophys. Res. Commun.* **2002**, *290*, 1441–1446.
- (6) Muralidhara, B. K.; Prakash, V. *Indian J. Biochem. Biophys.* **2002**, *39*, 318–324.
- (7) Bhuyan, A. K. *Biochemistry* **2002**, *41*, 13386–13394.
- (8) Sinha, K. K.; Udgaonkar, J. B. *Proc. Natl. Acad. Sci.* **2008**, *105*, 7998–8003.
- (9) Rosgen, J.; Pettit, B. M.; Bolen, D. W. *Biophys. J.* **2005**, *89*, 2988–2997.
- (10) Nandel, F. S.; Verma, R.; Singh, B.; Jaina, D. V. S. *Pure Appl. Chem.* **1998**, *70*, 659–664.
- (11) Wetlaufer, D. B.; Malik, S. K.; Stoller, L.; Coffin, R. L. *J. Am. Chem. Soc.* **1964**, *86*, 508–514.
- (12) Dohnal, V.; Costas, M.; Carrillo-Nava, E.; Hovorka, S. *Biophys. Chem.* **2001**, *90*, 183–202.
- (13) Brandts, J. F. *J. Am. Chem. Soc.* **1964**, *86*, 4302–4314.
- (14) Frank, H. S.; Frank, F. J. *J. Chem. Phys.* **1968**, *48*, 4746–4757.
- (15) Abu-Hamdiyyah, M. *J. Phys. Chem.* **1965**, *69*, 2720–2725.
- (16) Soper, A. K.; Caster, E. W.; Luzar, A. *Biophys. Chem.* **2003**, *105*, 649–666.
- (17) Zou, Q.; Bennion, B. J.; Daggett, V.; Murphy, K. P. *J. Am. Chem. Soc.* **2002**, *124*, 1192–1202.
- (18) Rossky, P. J. *Proc. Natl. Acad. Sci.* **2008**, *105*, 16825–16826.
- (19) Tsumoto, K.; Ejima, D.; Kumagai, I.; Arakawa, T. *Protein Expression Purif.* **2003**, *28*, 1–8.
- (20) Gull, N.; Sen, P.; Kabir-ud-Din; Khan, R. H. *J. Biochem.* **2007**, *141*, 261–268.
- (21) Remmele, R. L. Jr., Microcalorimetric approaches to biopharmaceutical development. In *Analytical Techniques for Biopharmaceutical Development*; Rodriguez-Diaz, R., Wehr, T., Tuck, S., Eds.; Marcel Dekker: New York, NY, 2005; pp 327–381.
- (22) Roberts, C. J.; Darrington, R. T.; Whitley, M. B. *J. Pharm. Sci.* **2003**, *92*, 1095–1111.
- (23) Cromwell, M. E. M.; Hilario, E.; Jacobsen, F. *AAPS J.* **2006**, *8*, ES72–ES79.
- (24) Roberts, C. J. *Biotechnol. Bioeng.* **2007**, *98*, 927–938.
- (25) Privalov, P. L.; Khechinashvili, N. N. *J. Mol. Biol.* **1974**, *86*, 665–684.
- (26) Privalov, P. L. *Adv. Protein Chem.* **1979**, *33*, 167–241.
- (27) Halskau, O., Jr.; Perez-Jimenez, R.; Ibarra-Molero, B.; Underhaug, J.; Munoz, V.; Martinez, A.; Sanchez-Ruiz, J. M. *Proc. Natl. Acad. Sci. U.S.A.* **2008**, *105*, 8625–8630.
- (28) Naganathan, A. N.; Perez-Jimenez, R.; Munoz, V.; Sanchez-Ruiz, J. M. *Phys. Chem. Chem. Phys.* **2011**, *13*, 17064–17076.
- (29) Remmele, R. L., Jr.; Bhat, S. D.; Phan, D. H.; Gombotz, W. R. *Biochemistry* **1999**, *38*, 5241–5247.
- (30) Remmele, R. L., Jr.; Zhang-van Enk, J.; Dharmavaram, V.; Balaban, D.; Durst, M.; Shoshitaishvili, A.; Rand, H. *J. Am. Chem. Soc.* **2005**, *127*, 8328–8339.
- (31) Smith, R. R.; Charon, N. W.; Canady, W. J. *J. Phys. Chem.* **1989**, *93*, 5938–5943.
- (32) Ben-Naim, A. *J. Chem. Phys.* **1984**, *81*, 2016–2028.
- (33) Ben-Naim, A. *J. Phys. Chem.* **1978**, *82*, 792–803.
- (34) Harr, L.; Gallagher, J. S.; Kell, G. S. *NBS/NRC Steam Tables*; Hemisphere Publishing Corp.: New York, 1984.
- (35) Makhatadze, G. I.; Privalov, P. L. *J. Chem. Thermodyn.* **1988**, *20*, 405–412.
- (36) Baldwin, R. L. *Proc. Natl. Acad. Sci.* **1986**, *83*, 8069–8072.
- (37) Bohon, R. L.; Claussen, W. F. *J. Am. Chem. Soc.* **1951**, *73*, 1571–1578.
- (38) Hovorka, S.; Dohnal, V.; Carrillo-Nava, E.; Costas, M. *J. Chem. Thermodyn.* **2000**, *32*, 1683–1705.
- (39) Privalov, P. L.; Khechinashvili, N. N.; Atanasov, B. P. *Biopolymers* **1971**, *10*, 1865–1890.
- (40) Sanchez-Ruiz, J. M.; Lopez-Lacomba, J. L.; Cortijo, M.; Mateo, P. L. *Biochemistry* **1988**, *27*, 1648–1652.
- (41) Lepock, J. R.; Ritchie, K. P.; Kolios, M. C.; Rodahl, A. M.; Heinz, K. A.; Kruuv, J. *Biochemistry* **1992**, *31*, 12706–12712.
- (42) Luke, K.; Apiyo, D. Wittung-Stafshede. *Biophys. J.* **2005**, *89*, 3332–3336.
- (43) Ross, P. D.; Subramanian, S. *Biochemistry* **1981**, *20*, 3096–3102.
- (44) Norde, W.; Haynes, C. A. In *Protein at Interfaces II. Fundamentals and Applications*; Horbett, T. A., Brash, J. L., Eds.; American Chemical Society: Washington D.C., 1995; pp 26–40.
- (45) Privalov, P. L. Scanning microcalorimeters for studying macromolecules. *Pure Appl. Chem.* **1980**, *52*, 479–497.
- (46) Makhatadze, G. I.; Privalov, P. L. *J. Mol. Biol.* **1992**, *226*, 491–505.
- (47) Auton, M.; Bolen, D. W.; Rosgen, J. *Proteins* **2008**, *73*, 802–813.
- (48) Klimov, D. K.; Straub, J. E.; Thirumalai, D. *Proc. Natl. Acad. Sci.* **2004**, *101*, 14760–14765.
- (49) Lee, M.-E.; van der Vegt, F. A. *J. Am. Chem. Soc.* **2006**, *128*, 4948–4949.
- (50) Shimizu, S.; Chan, H. S. *Proteins: Struct., Funct., Genet.* **2002**, *49*, 560–566.
- (51) Muller, N. *J. Phys. Chem.* **1990**, *94*, 3856–3859.
- (52) Vanzo, F.; Madan, B.; Sharp, K. *J. Am. Chem. Soc.* **1998**, *120*, 10748–10753.
- (53) Teeter, M. M. *Proc. Natl. Acad. Sci.* **1984**, *81*, 6014–6018.

- (53) Kauzmann, W. *Nature* **1987**, 325, 763–764.
- (54) Tanford, C. In *The Hydrophobic Effect: Formation of Micelles and Biological Membranes*; John Wiley & Sons: New York, 1973.
- (55) Privalov, P. L.; Gill, S. J. *Pure Appl. Chem.* **1989**, 61, 1097–1104.
- (56) Gill, S. J.; Dec, S. F.; Olofsson, G.; Wadso, I. *J. Phys. Chem.* **1985**, 89, 3758–3761.
- (57) Southhall, N. T.; Dill, K. A.; Haymet, A. D. J. *J. Phys. Chem. B* **2002**, 106, 521–533.
- (58) Chandler, D. *Nature* **2005**, 437, 640–647.
- (59) Barone, G.; Giancola, C. *Pure Appl. Chem.* **1990**, 62, 57–68.
- (60) Zangi, R.; Zhou, R.; Berne, B. J. *J. Am. Chem. Soc.* **2009**, 131, 1535–1541.
- (61) OoI, T.; Oobatake, M.; Nemethy, G.; Scheraga, H. A. *Proc. Natl. Acad. Sci.* **1987**, 84, 3086–3090.
- (62) Privalov, P. L. In *Colloquium Mosbach. Protein Structure and Protein Engineering*; Winnacker, E.-L., Huber, R., Eds.; Springer-Verlag: Berlin Heidelberg, 1988; pp 6–15.
- (63) Neira, J. L.; Gomez, J. *Eur. J. Biochem.* **2004**, 271, 2165–2181.
- (64) Stumpe, M. C.; Grubmuller, H. *Biophys. J.* **2009**, 96, 3744–3752.